communications materials

Article

https://doi.org/10.1038/s43246-024-00502-7

High-frequency low-dielectric-loss in linear-backbone-structured polyimides with ester groups and ether bonds

Chenggang Zhang[1], Xiaojie He[1] & Qinghua Lu[2,3,4] ✉

Polyimides have emerged as promising dielectric materials for communication equipment, owing to their excellent thermal stability and processability. Nonetheless, a pressing need remains to reduce the high-frequency dissipation factor (D_f) of polyimides. Here, we synthesized various polyimides featuring linear backbone structures, finding that polyimides that incorporate a combination of ester groups and ether bonds exhibit low D_f values of 0.0015-0.0024 at 10 GHz. Even in high humidity and temperature conditions they maintain low D_f values of <0.005 at 10 GHz. To gain insight into the factors influencing this behavior, we conduct a comprehensive study involving aggregation structures and hygroscopic properties. Our findings highlight the pivotal role of high orientation and crystallinity in determining the high-frequency D_f of polyimide films.

In the current era of rapid advancements in internet technology, high-speed and high-frequency communication devices have seen a meteoric rise in prominence. For this purpose, the dielectric material with a low signal propagation loss rate (L) is proposed[1,2]. The L value of electronic equipment depends strongly on the dielectric constant (D_k) and dielectric loss (D_f) of the used polymer materials, as elucidated by the modified Maxwell's equation[3,4]: $L \propto f\, D_f \sqrt{D_k}$. With signal transmission frequencies surpassing the 10 GHz threshold, the performance criteria for dielectric materials have grown considerably stringent, especially dielectric loss (D_f)[5,6].

Polymers are the most critical dielectric material and have gained widespread adoption[7]. Among multitudinous dielectric polymers, polyimide (PI) has enjoyed extensive applications in communication technology for several years[8,9]. It has been widely used in flexible printed circuit boards (PCBs) and organic electronic devices due to its commendable dielectric properties, exceptional thermal stability, ease of processing, and flexibility in designing its molecular structure[10,11]. Nonetheless, following the development of communication technology, current commercial-grade PIs are unable to afford further high-frequency and speed electronic signals, impairing the transportation of signals in higher frequency[12]. PI's intrinsic design flexibility and processability provide an avenue for structural modifications, thereby enabling the effective enhancement of its performance. Currently, prevalent approaches to diminish D_k involve strategies such as augmenting the overall free volume (utilizing extended side chains[13], adopting noncoplanar structures[14–16], etc.), reducing the molecular chain's polarity (via −F, $-CF_3$ modifications[17,18], etc.), or introducing low-D_k fillers (constructing porous structures[19,20], introducing fluorographene[21–23], etc.). Numerous effective strategies exist for lowering D_k, and the associated theories have attained a relatively advanced stage of development. In contrast, the methodologies and theories about D_f, the more critical parameter in signal transmission, remain less well-defined[24,25]. D_f results from dielectric relaxation under alternating electric fields and energy dissipation due to the rotation of polarization units[26,27]. Consequently, the approach to mitigating dielectric loss revolves around preventing polarization unit rotation at varying frequencies, focusing on inhibiting dipole moment polarization and electronic polarization[28].

High-frequency dielectric materials, such as liquid crystal polymers (LCP)[29,30], typically exhibit linear and highly crystalline polymer structures. Consequently, a straightforward approach[31,32] is to engineer linear, low-free-volume structures with inherent rigidity to attain pronounced orientation. Linear functional groups, including ether bonds, carbonyl groups, amide bonds, and ester groups[33,34], emerge as the preferred choice for linear backbone chains of PIs. Japanese scholars[5,32] have discovered that the introduction of ester groups can effectively reduce D_f. They attempted to enhance molecular chain rigidity by introducing ester structures with benzene rings and biphenyl, and the synthesized PI exhibited a dielectric loss of less than 0.005. This theory guided us to prepare PIs with full-ester structures for low D_f. Nevertheless, the full-ester PIs have been found to have the disadvantage of brittleness due to excessive rigidity[35]. Based on the result,

[1]School of Chemical Science and Engineering, Tongji University, Siping Road No. 1239, 200092 Shanghai, China. [2]School of Chemistry and Chemical Engineering, Shanghai Jiao Tong University, Dongchuan Road No. 800, 200240 Shanghai, China. [3]Shanghai Key Lab of Electrical & Thermal Aging, Shanghai Jiao Tong University, Dongchuan Road No. 800, 200240 Shanghai, China. [4]State Key Laboratory of Metal Matrix Composites, Shanghai Jiao Tong University, Dongchuan Road No. 800, 200240 Shanghai, China. ✉e-mail: qhlu@sjtu.edu.cn

we postulated that a linear molecular chain framework combining rigid and flexible segments may improve the brittleness of PI films while accelerating a more uniform orientation of PI chains, constraining internal motion, thereby diminishing D_f.

To this end, we compared the aggregation and dielectric properties of three series of polyimides: polyetherimide series (PEIs) with flexible double-ether bonds (ODA-ODPA), three-ether bonds (TPE-Q-ODPA, ODA-HQDPA), or carbonyl-ether combination (A1C-ODPA), polyimide series (PIs) with the combination of mono ether bonds and rigid benzene ring in diamine or dianhydride (PDA-ODPA, ODA-PMDA), as well as poly-ester-ether imide series (PEsIs) with a combination of flexible and rigid segments, which contains 1–2 ester groups (A1E-ODPA, A2EB-ODPA and ODA-TA2EB) in diamine or dianhydride, respectively. Among these variations, the polyimides comprising ester groups and ether bonds (PEsIs) exhibited the most impressive attributes regarding thermal stability, dielectric properties, and water absorption. The reasons behind these outstanding characteristics are examined comprehensively by analyzing the impact of functional group modifications. The remarkable low-dielectric-loss properties primarily stem from the high orientation and dense packing of PEsIs. These factors effectively constrain the localized motions of the rigid and linear backbone structure during rapid frequency fluctuations. In addition, PEsIs (A2EB-ODPA and ODA-TA2EB) demonstrate an impressively low moisture absorption rate (~0.72% and 0.88%, respectively), safeguarding the stability of their low-dielectric-loss properties in diverse humid environments. Our approach offers a straightforward design solution for achieving inherently low-dielectric-loss polyimides and holds promise for broader applications across other polymer systems. This innovation can potentially drive significant advancements in the field of microelectronics.

Results and discussion

Characterization and aggregation structure of PEsIs

All PIs were synthesized by a two-step process: polycondensation and thermal imidization. To facilitate a comprehensive investigation of PEsIs, PIs with different functional groups were prepared using an identical methodology, as shown in Fig. 1a. In addition to the molecular structures in Fig. 1c, other alternative structures were explored, as documented in Supplementary Table 1. However, these complementary structures could not yield intact polyimide films due to the reactivity, solubility, and rigidity of ester-based monomers[35]. The M_w values of the PEsIs (Supplementary Table 2) are in the range of 5.69–11.79, which are lower than that of PIs (ODA-PMDA and PDA-ODPA). The main reason should be attributed to the activity of ester monomers, while PEsIs still form films (the images of PEsIs are shown in Supplementary Fig. 1). The ATR-FTIR spectra prove the complete imidation of PEsIs and PIs (Supplementary Fig. 2 and Supplementary Discussion 1).

For polymers, the aggregation structure of the polymer can affect their physical properties by modulating the mobility of their molecular segments. Figure 2a–c shows the XRD patterns of the PEsIs, PEIs, and PIs. In contrast to the singular amorphous peaks of PEIs, the XRD spectra of PEsIs marked with red ester bond in the diagram exhibit a distinctive pattern comprising both crystalline and amorphous peaks. For a given dianhydride ODPA, A1E-ODPA displays a crystalline property, distinguishing it from counterparts ODA-ODPA with ether bond and A1C-ODPA with carbonyl bond (Fig. 2a). The combination of carbonyl-ether or ether-ether (double flexible combination) does not induce significant orientation or crystallinity in the polyimide chains. Although PDA-ODPA with a combination of a rigid benzene ring and flexible ether bond also shows some crystallinity, the relatively poor crystallinity as verified by the Polarized Optical Microscope image (POM), as shown in Fig. 2d. The performance of PDA-ODPA is inferior to that of PEsIs, which would be proven in subsequent performance studies, so the structure did not be studied specifically. The definitions of flexible and rigid segments are based on existing knowledge and the fact that the T_gs of PEsIs are significantly elevated after the introduction of ester bonds in PI backbones (for DMA curves see Supplementary Fig. 3). The same pattern is observed with A2EB-ODPA (Fig. 2b) and ODA-TA2EB (Fig. 2c). A1E-ODPA, A2EB-ODPA, and ODA-TA2EB films exhibit multiple peaks with high intensity, and their crystallinities are 17.4%, 28.6%, and 20.4%, respectively, according to the fitting of the peaks (details in Supplementary Discussion 2, Supplementary Fig. 4 and Supplementary Table 3). So far, we can draw the conclusion that the combination of the ester group, benzene ring, and imide ring serves as the rigid component in the polyimide backbone, and the ether bond segments function as the flexible element, this unique combination can effectively promote the orientation of the molecular chain (the experimental details are shown in Supplementary Discussion 3, Supplementary Tables 3, 4 and Supplementary Figs. 5–7). Compared to full-ester PIs (for POM see Supplementary Fig. 8), the distribution of crystalline regions in PEsIs is more uniform, which can effectively improve mechanical defects caused by uneven crystalline distribution.

Figure 2d shows the POM images of PEsIs and PIs. PEsIs have prominent and dense spherulite structures, and PDA-ODPA with rigid parts also has fewer spherulites, consistent with XRD. There is another crystallization phenomenon of TPE-Q-ODPA, but the performance is not improved. PEsIs are in the partially crystalline state rather than the liquid crystal state, as there are no crystalline peaks in the DSC curve (Supplementary Fig. 9). ODA-TA2EB exhibits a secondary relaxation within temperatures below 300 °C in the DSC curve. In comparison, the secondary relaxations of A1E-ODPA and A2EB-ODPA occur at temperatures exceeding 350 °C. All the above results prove again that the combination of ester groups and ether bonds is beneficial to the orderly stacking of the molecular chains.

To further understand the molecular aggregation structure of PEsIs films, a Molecular Dynamics (MD) simulation was also executed (see Supplementary Discussion 4 and Supplementary Fig. 10 for a detailed calculation process); some important structural parameters obtained from the calculation are listed in Table 1. All PEsIs (A1E-ODPA, A2EB-ODPA, and ODA-TA2EB) possess high R_g (44.26, 50.05, 46.66 Å) and A_{fr} (3.05, 3.61, 3.95 Å) compared to PEIs and PIs, which reflect the rigidity of molecular chains. The decrease in R_g and A_{fr} corresponds to enhanced chain flexibility[36]. This observation suggests that incorporating ester groups and ether bonds led to a more structured and less convoluted polymer chain conformation. Compared with full-ester PI with R_g (53.23 Å) and A_{fr} (6.23 Å)[35], PEsIs are more flexible, resulting in a more uniform crystallization area and elevated film toughness. Concurrently, the increase in the number of ester groups leads to more organized polymer chain conformations (A2EB-ODPA ~ ODA-TA2EB > A1E-ODPA). Cohesive Energy Density (CED) is the energy required to overcome the intermolecular force of vaporization of 1 mol of aggregates per unit volume[37], and in the cases of A2EB-ODPA and ODA-TA2EB, their CED values exhibit a noteworthy increase compared to those of PIs. This enhancement in intermolecular forces can be attributed to the synergistic effect arising from the presence of ester groups and ether bonds, potentially mitigating dipole deflection within the electric field. The influence of a solitary ester group, as exemplified by A1E-ODPA, on the polyimide molecular chain appears limited, one more ester bond in A2EB-ODPA increases the rigidity of molecular chains, thus enhancing the close packing between molecular chains, and thus A2EB-ODPA showing higher CED than that of A1E-ODPA. In contrast to other PIs, PEsIs exhibit a notable reduction in Fractional Free Volume (FFV)[38], the critical factor influencing D_k and D_f. This observation provides evidence that the aggregate structures within PEsIs films are densely packed, and the characteristic attributes to the synergy between ester groups and ether bonds. Collectively, these factors are likely to exert a pronounced influence on film performance, particularly dielectric properties.

The relationship between dielectric properties and aggregation structure of PEsIs films

For high-frequency communication, the dielectric properties of materials are the key factors to ensure high-speed signal transmission. Figure 3a shows D_k and D_f values of PEsIs and PIs films at 10 GHz. It is evident that PEsIs exhibit relatively low D_f values, and the D_f values of A1E-ODPA,

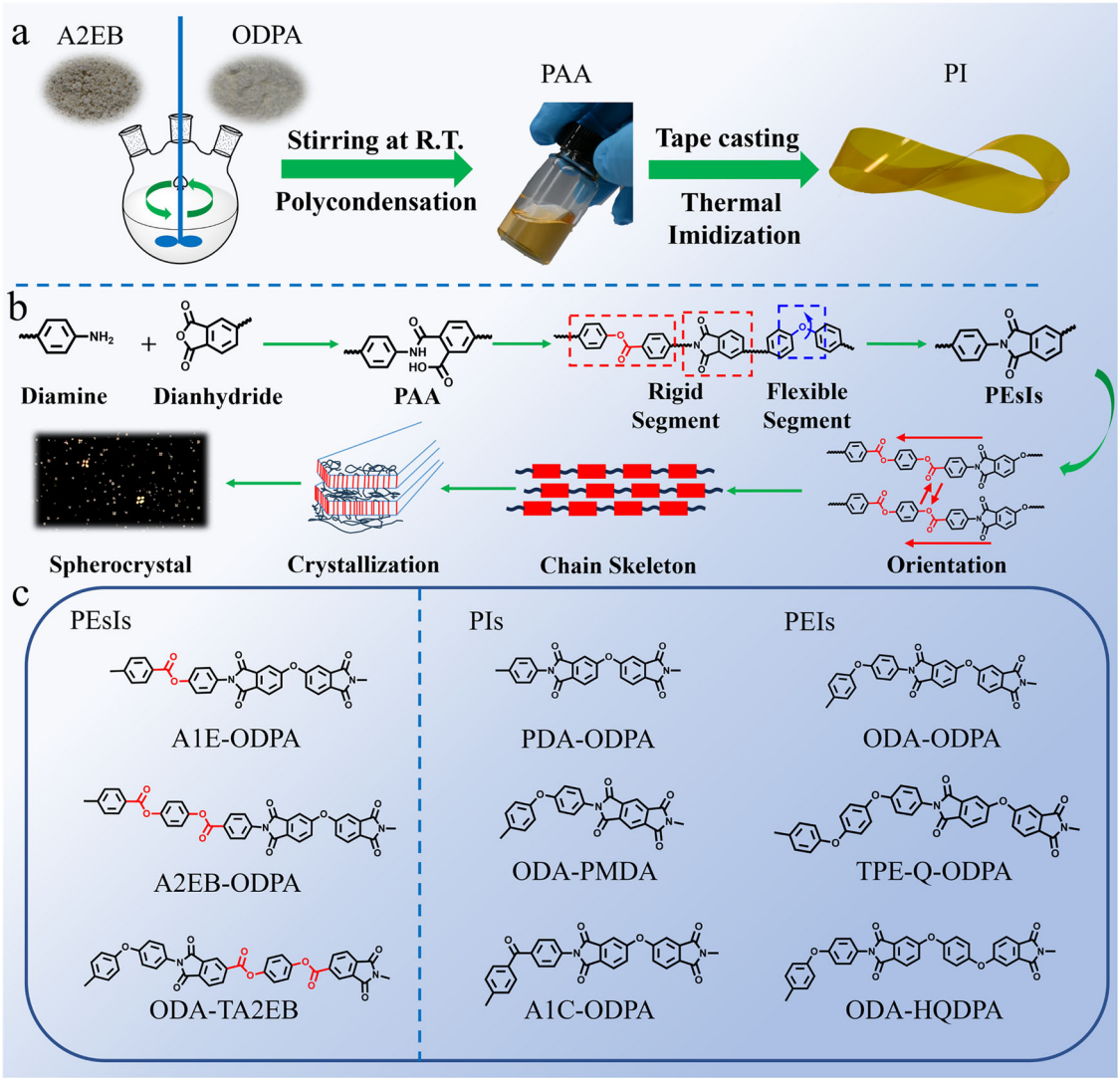

Fig. 1 | Schematic diagram of polyimide polymerization. a Synthesis of polyimides containing ester groups. **b** Microstructure diagram of the polymerization process and PEsIs. **c** The structural units of the PEsIs and PIs.

A2EB-ODPA, and ODA-TA2EB are 0.0024, 0.0015, and 0.0018, respectively. This low D_f can be ascribed to the restriction of dipole moment rotation, which results from the densely packed molecular chains and intermolecular interactions (Fig. 3b, c). The D_k values of PEsIs are in the range of 3.24 to 3.27. D_k of PIs is strongly correlated with the volume polarization (α/V) and the free volume (FFV). Consequently, the simultaneous presence of high α/V and low FFV in PEsIs contributes to their moderate D_k values (~3.26). It is worth noting that D_f and D_k exhibit distinct behaviors when atoms and groups are similar[13,31,35]; that is, lower D_f values may correspond to higher D_k values in instances when the polarity of functional groups is not significantly different. In simple terms, strong intermolecular interaction and a restricted free volume contribute to low D_f. In contrast, a low volume polarization rate and a large free volume indicate low D_k.

To further understand the exceptional dielectric property of the PEsIs, their wide-frequency dielectric spectra were systematically tested (Fig. 4a, b). The D_k of both PEsIs and PIs gradually declined as the frequency increased, owing to the frequency-dependent variation of dipole moments. In contrast to the behavior of D_k, D_f demonstrates a tendency to rise and then decline with increasing frequency. For instance, peak D_f values are observed for A2EB-ODPA and ODA-TA2EB at frequencies of 3.0×10^5 Hz and 5.2×10^5 Hz, respectively. The dielectric behavior of PEsIs at high and low frequencies resembles that of LCP[39,40]. Specifically, the D_f is relatively high at low frequencies and extremely low at high frequencies. If the concept of secondary relaxation is introduced into a frequency-dielectric spectrum, it can elucidate the higher dielectric loss observed in PEsIs at low frequencies compared with PIs. At low frequencies, the ester groups and their dipole moments within the main chain of PEsIs exhibit limited localized motion, resulting in "secondary dielectric relaxation" and high D_f. With increasing frequency, the limitation on the movement of dipole moments heightens and some dielectric relaxation fade away, which are primarily attributable to the elevated orientation of PEsIs. This boosted orientation directly results from the synergistic combination of ester groups and ether bonds. To gain deeper insights into the correlation between dielectric properties at both high and low frequencies (the details were in Supplementary Discussion 5), the relaxation times (τ) of polarization were calculated in the frequency range of 500 Hz to 1 MHz using the Debye equation, as shown in Fig. 4c and Supplementary Fig. 11. Obviously, there is a negative correlation between τ and D_f, meaning that higher τ values resulted in lower D_f values. The pronounced orientation observed in PEsIs significantly contributes to the increase in τ, further reducing D_f. Consequently, the strategic design of structures that amalgamate rigidity and flexibility to enhance molecular chain orientation and crystallinity holds promise for minimizing D_f. To expand the research scope, the dielectric properties of PEsIs were compared with those of polyimides in previous literature (Fig. 4d). The high-frequency

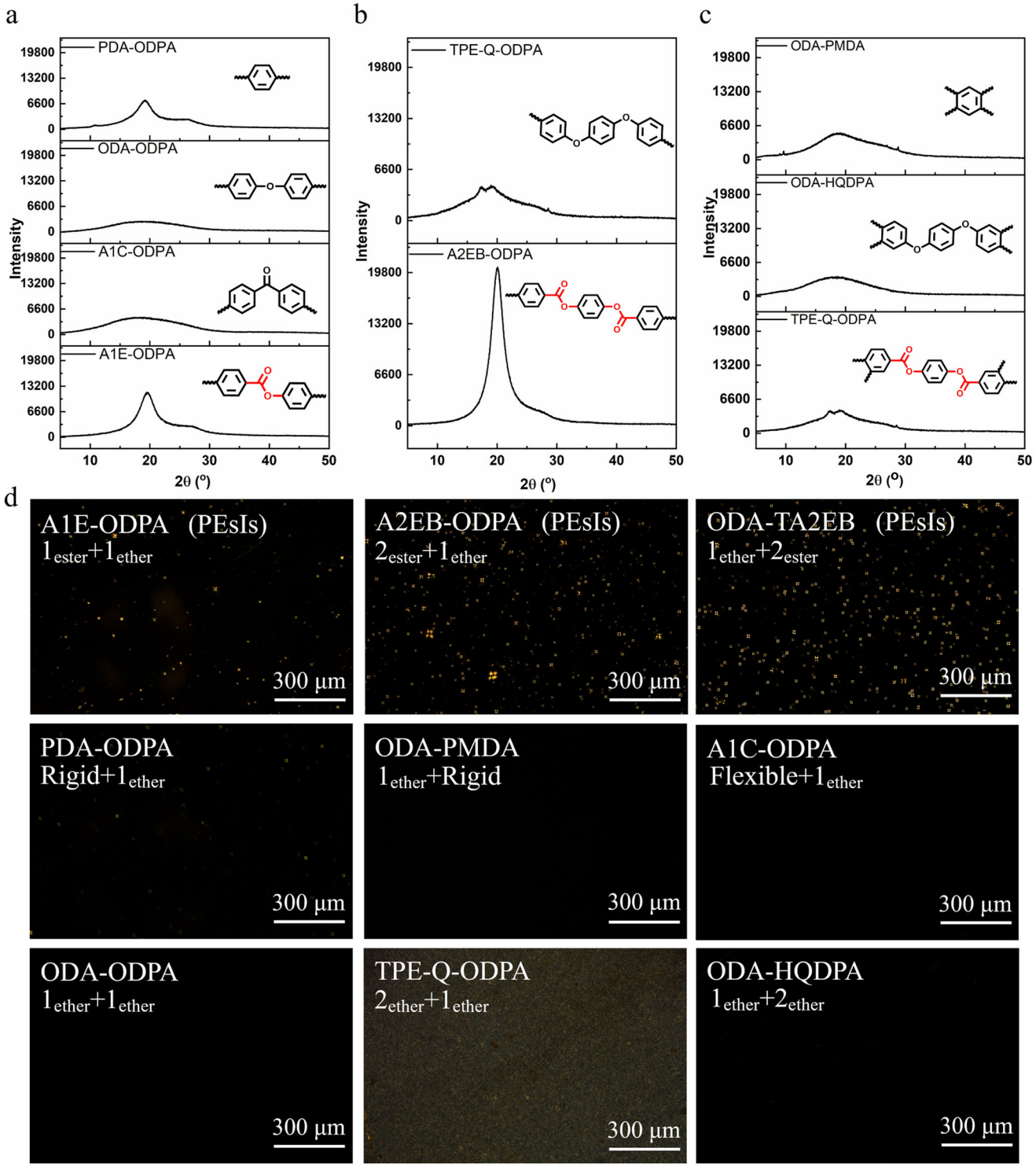

Fig. 2 | Characterization of aggregation structure. a XRD patterns of PDA-ODPA, ODA-ODPA, A1C-ODPA, and A1E-ODPA films. **b** TPE-Q-ODPA and A2EB-ODPA films. **c** ODA-PMDA, ODA-HQDPA and ODA-TA2EB. **d** POM images of PEsIs and PIs films.

dielectric performance of polyimides follows the trend before, even with the introduction of alicyclic or fluorinated groups. That is, D_k and D_f exhibit an opposite trend due to the aggregated structures of the polymers. Full-ester PIs also have low D_f due to the oriented crystallization of rigid molecular chains[35]. PEsIs take a step further than full-ester PI by connecting the rigid parts through ether bonds, resulting in a more evenly distributed crystallization zone and improving the overall performance of the films (for schematic diagram see Supplementary Fig. 12).

The relationship between dielectric properties and water absorption of PEsIs films

For dielectric materials, maintaining low water absorption is critical to ensure the stability of their dielectric properties[41]. From the water contact angle (Supplementary Fig. 13), PEsIs films have relatively lower water wettability than PI films (including PEIs). In Fig. 5a, the water absorption behaviors of PEsIs and PIs are investigated under various humidity conditions (Supplementary Table 5). Obviously, when

Table 1 | Computational results of the PEsIs, PIs and PEIs

	PI	R_g [a] (Å)	A_{fr} [b] (Å)	CED [c] (J cm^{-3})	FFV[d] (%)	Dipole moment (*D*)	α/V [e] (a.u.× mol cm^{-3})
PEsIs	A1E-ODPA	44.26	3.05	455.4	19.86	2.8736	1.007
	A2EB-ODPA	50.05	3.61	485.6	19.55	1.1249	1.029
	ODA-TA2EB	46.66	3.95	502.6	18.37	2.2580	1.029
PIs	PDA-ODPA	33.06	2.46	479.3	21.27	1.1829	0.971
	ODA-PMDA	35.27	3.71	478.1	22.57	1.5372	0.952
	A1C-ODPA	38.8	2.67	482.2	20.53	4.1309	1.010
PEIs	ODA-ODPA	33.79	2.32	445.4	22.07	0.9081	0.977
	TPE-Q-ODPA	36.99	1.68	363.8	21.02	1.4502	0.998
	ODA-HQDPA	36.47	2.15	426.0	21.11	1.1569	0.997

[a]Radius of Gyration.
[b]Kuhn segment length.
[c]Cohesive energy density.
[d]Fractional free volume, FFV = (V−1.3 V_W)/*V*.
[e]Volume polarizability.

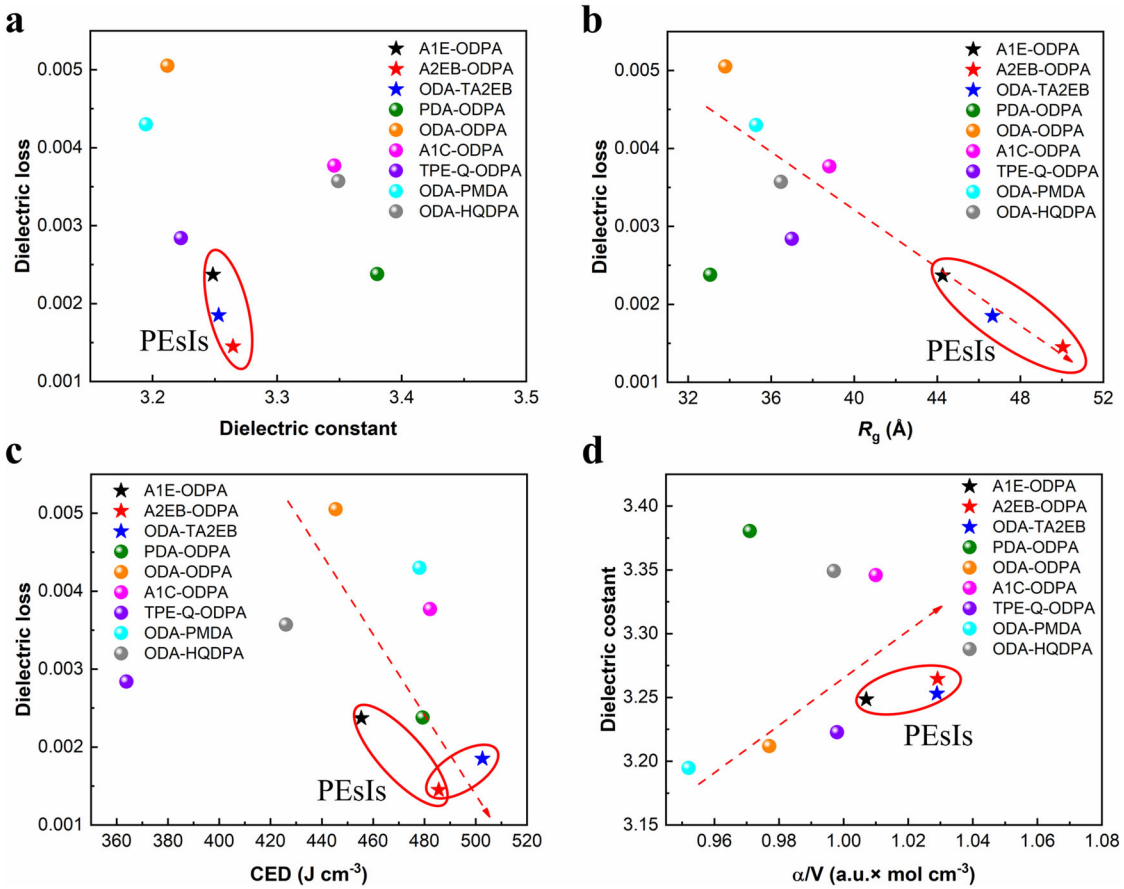

Fig. 3 | Factors affecting dielectric properties. a Relationship of D_k and D_f at 10 GHz. **b** Relationship of D_f and R_g. **c** Relationship of D_f and CED. **d** Relationship of D_k and α/V.

compared to PIs, PEsIs (A1E-ODPA, A2EB-ODPA, and ODA-TA2EB) exhibit significantly lower water absorption values of 0.97%, 0.72%, and 0.88%, respectively. The reasons for the low hygroscopic properties of PEsIs can be attributed to the more hydrophobic properties of ester groups than that of the imide bond, and the tightly arranged aggregation structure restricting the intrusion of water molecules[5,42]. To comprehensively elucidate the correlation between hygroscopicity and dielectric properties, D_k and D_f of PEsIs and PIs were measured at 10 GHz under varying conditions, including dry air, humid air, and subsequent water immersion (Fig. 5b and Supplementary Fig. 14). Notably, the D_f values of PEsIs exhibit minimal variation with changing humidity levels, especially in the case of A2EB-ODPA and ODA-TA2EB, which retain D_f values below 0.005 (0.0042 and 0.0041 at 10 GHz, respectively) even after water immersion. Due to the low water absorption, PEsIs exhibit a more minor increase in D_k than other PIs, with the increment falling within the range of 3% to 7%. Figure 5c–f directly depicts the significant

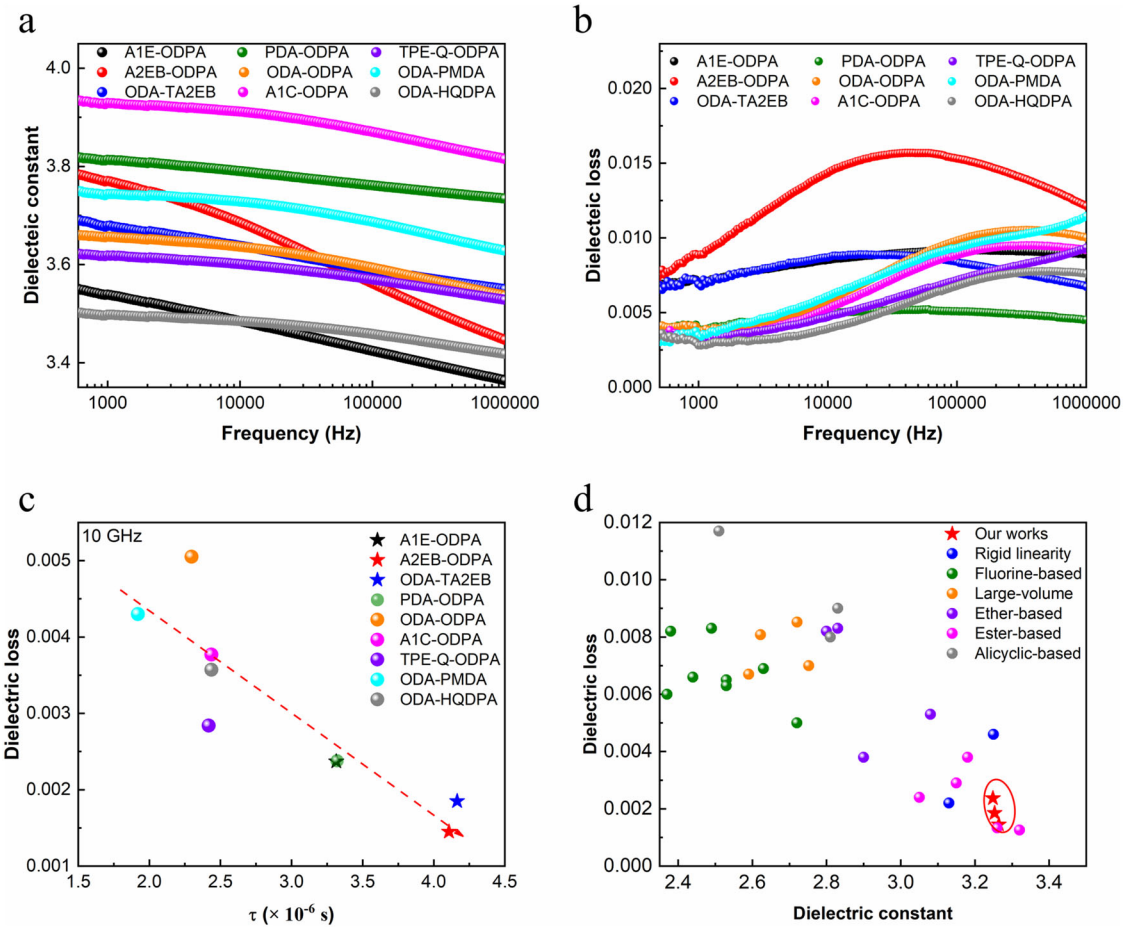

Fig. 4 | The relationship between high and low-frequency dielectric properties. Frequency dependence of D_k (**a**) and D_f (**b**) of PEsIs and PIs. **c** Relationship between τ and D_f of PEsIs and PIs at 10 GHz. **d** Comparison of dielectric properties at 10 GHz with other reported PIs[9,31,33,35,45–52].

correlation between dielectric properties and moisture absorption at 60% R.H. and in H_2O, respectively. Specifically, D_f and D_k of similar functional group-containing PIs are primarily influenced by their hygroscopic characteristics under high humidity conditions. Therefore, designing low moisture-absorbing structures is one of the directions for designing low-dielectric polymers. Compared to commercial PIs like ODA-PMDA, PEsIs are better suited for applications in challenging environments owing to their superior dielectric stability and low moisture absorption.

Thermal stability, mechanical properties, and electric breakdown of PEsIs films

Thermal properties of PIs are essential factors affecting their applications. DMA, TGA, and TMA were used respectively to characterize their glass transition temperature (T_g), thermal decomposition temperature (T_d), and coefficient of thermal expansion (CTE) (for TGA and TMA curves, see Supplementary Fig. 15), and the relevant data are listed in Table 2. PEsIs exhibit superior heat resistance compared to PIs, albeit with a slightly lower T_d. The high T_gs of PEsIs are mainly due to the rigidity of the molecular chain and the regularity and crystallization of the aggregate structure. However, the ester groups in PEsIs are more easily decomposed than other bonds at high temperatures above 470 °C, thereby resulting in a slightly low T_d. The secondary relaxation temperatures for A1E-ODPA, A2EB-ODPA, and ODA-TA2EB are 360 °C, 365 °C, and 228 °C, respectively, which result from the localized motion of ester groups within the low-frequency range. In a word, PEsIs performance are stable over a wide temperature range. In general, D_k and D_f of PIs decrease with temperature increasing due to the water loss in the films; however, the D_k and D_f of A2EB-ODPA and ODA-TA2EB can remain relatively stable vales with a small change at 10 GHz (Fig. 6), thereby rendering them well-suited for a broad spectrum of temperature environments. In the realm of flexible printed circuit boards (FPC)[43], one crucial parameter for dielectric materials is their CTE, which ideally should be equal to or lower than that of copper (17 ppm K^{-1}). Notably, the CTE value of A2EB-ODPA (7 ppm K^{-1}) is considerably lower than that of ODA-TA2EB (29 ppm K^{-1})[44]. The flexible segments positioned on different monomers (dianhydrides or diamines) thus exhibit differential effects on the thermal deformation of polyimides. Specifically, the thermal deformation decline of PEsIs with ether bonds in diamines is more significant than that in dianhydrides, and the principle holds for ODA-PMDA and PDA-ODPA.

The stress-strain curves of the PI films were tested (Supplementary Fig. 16), and the corresponding mechanical properties, including the tensile strength, initial modulus, and elongation at break, are listed in Table 2. Incorporating ester groups and ether bonds contributes to increasing PI's tensile strengths and modulus. This enhancement can be attributed to the in-plane orientation and dense packing of the molecular chains. The enhancement pattern in mechanical strength is similar to that of CTE; the strengthening effect is more pronounced when ester groups are present in diamines. Conversely, the elongation at break exhibits an opposite trend, and ε of ODA-TA2EB is greater than that of A2EB-ODPA. Additionally, the high orientation and dense packing increase the breakdown strength of PEsIs, surpassing 365 MV m^{-1}. This observation further underscores the significant role of high orientation through ester groups and ether bonds in enhancing insulation properties.

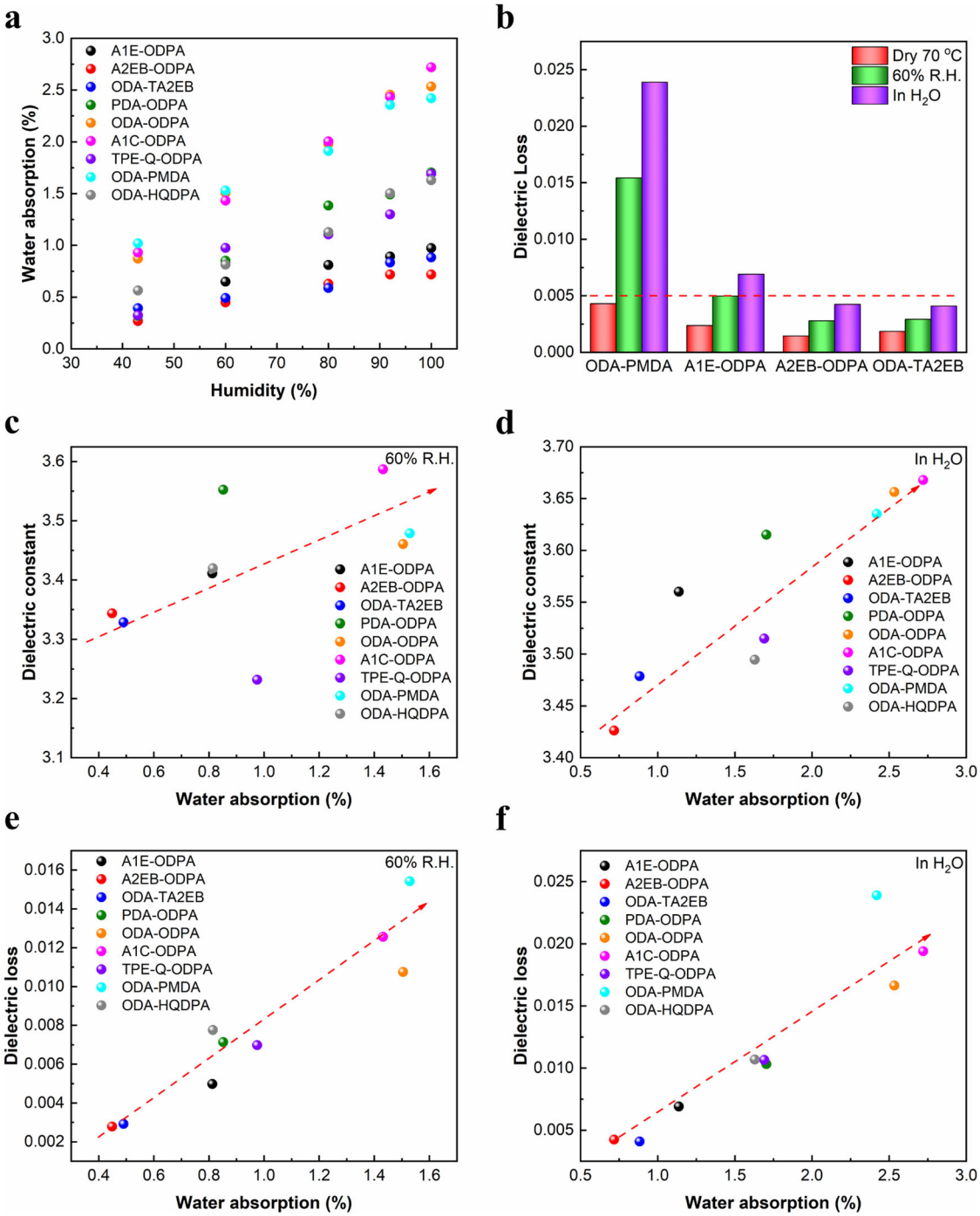

Fig. 5 | Relation between water absorption and dielectric loss. a The water absorption of PEsIs and PIs at different humidities. **b** D_f of ODA-PMDA, A1E-ODPA, A2EB-ODPA, and ODA-TA2EB at different humidities. The relationship between water absorption and D_k at 60% R. H. (**c**) and after soaking water (**d**). The relationship between water absorption and D_f at 60% R. H. (**e**) and after soaking water (**f**).

Conclusion

In summary, by incorporating simple ester and ether functional groups into the polyimide molecular chain skeleton, without the introduction of overly complex groups, we have uncovered a significant correlation between the aggregated structure and the properties of polyimides, particularly in terms of water absorption and high-frequency D_f. The discovery is of particular significance that combining ester groups, and ether bonds can effectively enhance chain orientation and induce crystallization in polyimides, substantially reducing their D_f. Specifically, A2EB-ODPA and ODA-TA2EB exhibited remarkably low D_f values (0.0015 and 0.0018, respectively) at 10 GHz, and these D_f values could be consistently maintained at a low level (<0.0045) even in high humidity environments. This remarkable phenomenon can be attributed to the restriction of dipole moment rotation and the prolongation of relaxation time achieved through the high orientation and crystallization of PEsIs. This effect is performed on the molecular chain level through the dense stacking of molecular chains and strong intermolecular interactions. Furthermore, the combination of ester groups and ether bonds played a crucial role in enhancing the thermal, electrical, and mechanical properties of PEsIs. Indeed, other properties of polyimides, including D_k and ε, warrant further investigation. Consequently, there is a pressing and captivating challenge within the realm of low-dielectric polymers, both from a

Table 2 | Thermal properties, mechanical properties and electric breakdown of PEI films

PI	T_g [a] (°C)	CTE [b] (ppm K^{-1})	$T_d^{5\%}$ [c] (°C)	$T_d^{10\%}$ [d] (°C)	R_w [e] (%)	σ [f] (MPa)	E [g] (GPa)	ε [h] (%)	E_b [i] (MV m^{-1})
A1E-ODPA	480	17	498	567	49.98	122 ± 2	2.4 ± 0.1	5 ± 1	365
A2EB-ODPA	480	7	491	552	47.05	173 ± 3	3.5 ± 0.1	8 ± 2	463
ODA-TA2EB	424	29	469	554	47.29	144 ± 2	1.9 ± 0.1	14 ± 2	374
PDA-ODPA	360	21	550	515	59.36	116 ± 1	2.3 ± 0.1	5 ± 1	320
ODA-PMDA	414	56	577	545	58.16	120 ± 2	1.1 ± 0.1	48 ± 5	332
A1C-ODPA	291	47	532	506	60.75	124 ± 1	1.5 ± 0.1	16 ± 2	194
ODA-ODPA	283	51	530	545	59.07	119 ± 2	1.5 ± 0.1	46 ± 4	307
TPE-Q-ODPA	263	57	522	589	55.94	114 ± 2	1.5 ± 0.1	15 ± 2	246
ODA-HQDPA	248	60	527	480	56.49	103 ± 1	1.1 ± 0.1	30 ± 4	284

[a]Glass transition temperature determined by DMA.
[b]Measured with TMA in the temperature range of 100–200 °C.
[c]Temperatures at 5% weight loss.
[d]Temperatures at 10% weight loss.
[e]Residual weight retention when heated to 800 °C under N_2.
[f]Tensile strength.
[g]Initial modulus.
[h]Elongation at break.
[i]Breakdown strength.

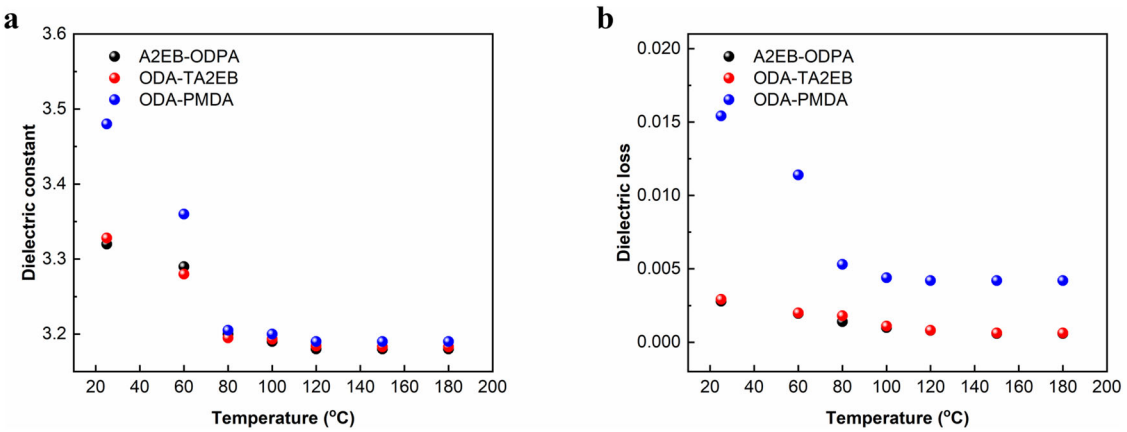

Fig. 6 | Relationship between temperature and dielectric loss. D_k (**a**) and D_f (**b**) of A2EB-ODPA, ODA-TA2EB, and ODA-PMDA at different temperatures at 10 GHz.

theoretical and practical standpoint. Our research endeavors can offer some insights and directions to address this challenge.

Methods

Materials

N, *N*-Dimethylacetamide (DMAc) was purchased from J&K Scientific Ltd, China. 4,4′-Diaminobenzophenone (A1C), Potassium Carbonate (K_2CO_3), Sodium Bromide (NaBr), Sodium Chloride (NaCl), and Potassium sulfate (K_2SO_4) were provided by Sinopharm Chemical Reagent Co. Ltd, China. 4,4′-Oxydianiline (ODA), *p*-PhenylenediaMine (PDA), Phenol, 4-amino-,1-(4-aminobenzoate) (A1E), 4,4′-[1,4-Phenylenebis(oxy)] bis[benzenamine] (TPE-Q), Pyromellitic dianhydride (PMDA), 1,4-Benzenediol,1,4-bis(4-aminobenzoate) (A2EB), *p*-Phenylene bis(trimellitate anhydride) (TA2EB), 1,4-Bis(3,4-dicarboxyphenoxy) benzene dianhydride (HQDPA) were purchased from Chinatech Chemical Co. Ltd, Tianjin, China and were used without further purification. All materials were used as received.

Preparation of polyimide films

A conventional two-step method was used for polyimide preparations (Fig. 1a). In a three-necked flask, diamine (5.0 mmol) was added to 15 mL of DMAc and stirred for 30 min under N_2 at room temperature. Then, dianhydride (5.0 mmol) was gradually added to this solution with continuous stirring (24 h) at room temperature until the reaction mixture turned to a viscous/clear poly(amic acid) (PAA) solution, and its viscosity was stabilized. The PAA solution was subsequently coated uniformly on a clean and dry glass plate with a controlled film thickness, and the solvent was removed in a vacuum oven at 100 °C. Then the PAA was thermally imidized with the temperature program of 250 °C (1 h)/300 °C (1 h)/330 °C (1 h) to produce the polyimide films. By soaking in deionized water for a period of time, the polyimide films could be peeled off the substrate. The film thicknesses of the polyimide samples are in the range of 30 ~ 50 μm. The schematic diagram of the microscopic crystal polymer structure is shown in Fig. 1b, and the polyimide structural units are shown in Fig. 1c and Supplementary Table 1. Polyimides are designed as PEsIs series with ester and ether bonds and PI series with flexible ether–ether bonds, ether-carbonyl bonds or monoether bonds.

Characterization

The number-average (M_n) and weightaverage (M_w) molecular weights were obtained by HLC-8320GPC (TOSOH, Japan) using DMAc containing 0.03 mol L^{-1} LiBr and 0.03 mol L^{-1} H_3PO_4 as an eluent. Infrared spectra (FTIR) of PI films were obtained on a Nicolet 6700 FTIR spectrometer (PerkinElmer, Inc., USA) over the range 4000–500 cm^{-1} by accumulating 16 scans. Dynamic mechanical analysis (DMA) was performed on a TA Instruments Q800 (USA) under a nitrogen atmosphere at 5 °C min^{-1}. The

coefficient of thermal expansion (CTE) was determined using a TA Instruments Q400 analyzer (USA) under a nitrogen atmosphere at 5 °C min^{-1} between 100 and 200 °C from the second heating curves. Thermal decomposition temperature was performed using a PerkinElmer Pyris analyzer (USA) under nitrogen at 10 °C min^{-1}. The mechanical properties of film samples were tested on a CMT1104 universal electromechanical tester (SUST, China) at 5 mm min^{-1}. The PI films' wide-angle X-ray diffraction (WAXD) analysis was executed on a Rigaku Miniflex 600 with Cu Kα radiation (λ = 1.54 Å). The parameter 2θ was measured and collected in the 5°–50° range. The thermodynamic properties of films were characterized under a nitrogen atmosphere using a heating and cooling rate of 10 °C min^{-1} by Discovery DSC 250 (TA, USA). Polarized Optical Microscopy (POM) images were obtained by Leica DM LP (Leica, Germany). The moisture rate was measured using a precision electronic balance. The films were dried in an oven at 110 °C for 24 h and measured its weight (m_0). Then, the films were exposed to different humidity environments for 3 days, and their weights (m_n) were measured. Humidity is controlled by the specific saturated solution (the details are seen in Supplementary Table 5). The films were soaked in water at 30 °C for 3 days, and their weight (m_w) was measured. The moisture rate was calculated by the Eqs. (1), (2):

$$A_n(\%) = \frac{m_n - m_0}{m_0} \times 100\% \quad (1)$$

$$A_w(\%) = \frac{m_w - m_0}{m_0} \times 100\% \quad (2)$$

where A_n and A_w are the absorption ratios in the specific humidity and after soaking in water, respectively. The frequency-dielectric spectrums were measured 10 times by an Agilent instrument (E4980A, USA) in a frequency range of 10^2 Hz to 10^6 Hz at 23 °C and 50% relative humidity. The electrode area is 0.2827 cm^2 (diameter of 0.6 cm). The dielectric constant and dielectric loss at 10 GHz were measured by ENA 330 Network Analyzer E5080B (USA) at 23 °C and 40% relative humidity. The sample shape of the high-frequency dielectric test and breakdown strength is a square of 3 × 3 cm^2. The breakdown strength was measured by a high-temperature voltage breakdown measuring system (DDJ-50kv, China).

Data availability

The data that support the findings of this study are available from the corresponding author upon reasonable request.

Received: 16 December 2023; Accepted: 11 April 2024;
Published online: 17 April 2024

References

1. Zhao, W. et al. 2D Titanium carbide printed flexible ultrawideband monopole antenna for wireless communications. *Nat. Commun.* **14**, 278 (2023).
2. Liaw, D.-J. et al. Advanced polyimide materials: Syntheses, physical properties and applications. *Prog. Polym. Sci.* **37**, 907–974 (2012).
3. Yin, Y. et al. Transparent and flexible cellulose dielectric films with high breakdown strength and energy density. *Energy Storage Mater* **26**, 105–111 (2020).
4. Lei, X., Chen, Y., Qiao, M., Tian, L. & Zhang, Q. Hyperbranched polysiloxane (HBPSi)-based polyimide films with ultralow dielectric permittivity, desirable mechanical and thermal properties. *J. Mater. Chem. C* **4**, 2134–2146 (2016).
5. Hasegawa, M., Sakamoto, Y., Tanaka, Y. & Kobayashi, Y. Poly(ester imide)s possessing low coefficients of thermal expansion (CTE) and low water absorption (III). Use of bis(4-aminophenyl)terephthalate and effect of substituents. *Eur. Polym. J.* **46**, 1510–1524 (2010).
6. Hasegawa, M., Ishigami, T. & Ishii, J. Optically transparent aromatic poly(ester imide)s with low coefficients of thermal expansion (1). Self-orientation behavior during solution casting process and substituent effect. *Polymer* **74**, 1–15 (2015).
7. Zhang, C. et al. Flexible Cellulose/BaTiO3 Nanocomposites with High Energy Density for Film Dielectric Capacitor. *ACS Sustain. Chem. Eng.* **7**, 10641–10648 (2019).
8. Kaltenbrunner, M. et al. An ultra-lightweight design for imperceptible plastic electronics. *Nature* **499**, 458–463 (2013).
9. Li, Y. et al. Progress in low dielectric polyimide film—a review. *Prog. Org. Coat.* **172**, 107103 (2022).
10. Xia, X., He, X., Zhang, S., Zheng, F. & Lu, Q. Short-side-chain regulation of colorless and transparent polyamide-imides for flexible transparent displays. *Eur. Polym. J.* **191**, 112030 (2023).
11. Xiao, P. et al. Tailoring the microporosity and gas separation property of soluble polybenzoxazole membranes derived from different regioisomer monomers. *Sep. Purif. Technol.* **311**, 123340 (2023).
12. Fan, H. et al. Low-dielectric polyimide constructed by integrated strategy containing main-chain and crosslinking network engineering. *Polymer* **279**, 126035 (2023).
13. Liu, Y. et al. A Bulk Dielectric Polymer Film with Intrinsic Ultralow Dielectric Constant and Outstanding Comprehensive Properties. *Chem. Mater.* **27**, 6543–6549 (2015).
14. Xiao, P., He, X., Zheng, F. & Lu, Q. Super-heat resistant, transparent and low dielectric polyimides based on spirocyclic bisbenzoxazole diamines with Tg > 450 °C. *Polym. Chem.* **13**, 3660–3669 (2022).
15. Liu, Y. et al. High-performance functional polyimides containing rigid nonplanar conjugated triphenylethylene moieties. *Chem. Mater.* **24**, 1212–1222 (2012).
16. Zhou, Y., Zhang, S., Zheng, F. & Lu, Q. Intrinsically black polyimide with retained insulation and thermal properties: a black anthraquinone derivative capable of linear copolymerization. *Macromolecules* **54**, 9307–9318 (2021).
17. Baek, Y. et al. Fluorinated polyimide gate dielectrics for the advancing the electrical stability of organic field-effect transistors. *ACS Appl. Mater. Interfaces* **6**, 15209–15216 (2014).
18. He, J., Wu, X. & Cheng, Y. Low dielectric post-cured benzocyclobutene-functionalized fluorine-containing polyimide material. *Eur. Polym. J.* **196**, 112334 (2023).
19. Khim, S., Hwang, Y. C., Choi, J., Park, H. & Nam, K.-H. Temperature-invariant large broadband polyimide dielectrics with multimodal porous networks. *ACS Appl. Polym. Mater.* **5**, 4159–4169 (2023).
20. Chen, Y. et al. Nanoporous low-κ polyimide films via poly(amic acid)s with grafted poly(ethylene glycol) side chains from a reversible addition–fragmentation chain-transfer-mediated process. *Adv. Funct. Mater.* **14**, 471–478 (2004).
21. Ramani, R. et al. Free volume study on the origin of dielectric constant in a fluorine-containing polyimide blend: poly(vinylidene fluoride-co-hexafluoro propylene)/poly(ether imide). *J. Phys. Chem. B* **118**, 12282–12296 (2014).
22. Zhang, Y., Wang, R., Zhang, X. & Guo, S. Ingenious sandwich-like adhesive films and controllable introduction of fluorine-containing groups toward strong adhesive strength and low dielectric characteristics. *Ind. Eng. Chem. Res.* **61**, 14494–14507 (2022).
23. Li, Y., Chen, T., Liu, Y., Liu, X. & Wang, X. Simultaneously enhance dielectric strength and reduce dielectric loss of polyimide by compositing reactive fluorinated graphene filler. *Polymer* **254**, 125084 (2022).
24. Wang, L., Yang, J., Cheng, W., Zou, J. & Zhao, D. Progress on polymer composites with low dielectric constant and low dielectric loss for high-frequency signal transmission. *Front. Mater.* **8** (2021).
25. Prateek, Thakur, V. K. & Gupta, R. K. Recent progress on ferroelectric polymer-based nanocomposites for high energy density capacitors:

synthesis, dielectric properties, and future aspects. *Chem. Rev.* **116**, 4260–4317 (2016).
26. Baer, E. & Zhu, L. 50th anniversary perspective: dielectric phenomena in polymers and multilayered dielectric films. *Macromolecules* **50**, 2239–2256 (2017).
27. Zhu, L. Exploring strategies for high dielectric constant and low loss polymer dielectrics. *J. Phys. Chem. Lett.* **5**, 3677–3687 (2014).
28. Qin, M., Zhang, L. & Wu, H. Dielectric loss mechanism in electromagnetic wave absorbing materials. *Adv. Sci.* **9**, 2105553 (2022).
29. Mucha, M. Polymer as an important component of blends and composites with liquid crystals. *Prog. Polym. Sci.* **28**, 837–873 (2003).
30. Urata, S., Hijiya, H., Niwano, K. & Matsui, J. Theoretical estimation of dielectric loss of oxide glasses using nonequilibrium molecular dynamics simulations. *J. Am. Ceram. Soc.* **105**, 4200–4207 (2022).
31. He, J.-J., Yang, H.-X., Zheng, F. & Yang, S.-Y. Dielectric properties of fluorinated aromatic polyimide films with rigid polymer backbones. *Polymers* **14**, 649 (2022).
32. Hasegawa, M., Saito, T. & Tsujimura, Y. Poly(ester imide)s possessing low coefficients of thermal expansion and low water absorption (IV): Effects of ester-linked tetracarboxylic dianhydrides with longitudinally extended structures. *Polym. Adv. Technol.* **31**, 389–406 (2020).
33. Chen, Y.-C. et al. Investigation of the structure–dielectric relationship of polyimides with ultralow dielectric constant and dissipation factors using density functional theory. *Polymer* **256**, 125184 (2022).
34. Xia, X., Zhang, S., He, X., Zheng, F. & Lu, Q. Molecular necklace strategy for enhancing modulus and toughness of colorless transparent polyimides for cover window application. *Polymer* **259**, 125358 (2022).
35. Zhang, C., He, X. & Lu, Q. Polyimide films with ultralow dielectric loss for 5G applications: Influence and mechanism of ester groups in molecular chains. *Eur. Polym. J.* **200**, 112544 (2023).
36. Mohammadi, M., Davoodi, J., Javanbakht, M. & Rezaei, H. Glass transition temperature of PMMA/modified alumina nanocomposite: molecular dynamic study. *Mater. Res. Express* **6**, 035309 (2019).
37. Scatchard, G. Equilibria in non-electrolyte solutions in relation to the vapor pressures and densities of the components. *Chem. Rev.* **8**, 321–333 (1931).
38. He, X., Zhang, S., Zhou, Y., Zheng, F. & Lu, Q. The "fluorine impact" on dielectric constant of polyimides: A molecular simulation study. *Polymer* **254**, 125073 (2022).
39. Plesu, R., Malik, T. M. & Prud'homme, R. E. Dielectric relaxation properties of linear polyesters derived from β-propiolactone. *Polymer* **33**, 4463–4469 (1992).
40. Kocakülah, G., Algül, G. & Köysal, O. Effect of CdSeS/ZnS quantum dot concentration on the electro-optical and dielectric properties of polymer stabilized liquid crystal. *J. Mol. Liq.* **299**, 112182 (2020).
41. Bei, R. et al. A systematic study of the relationship between the high-frequency dielectric dissipation factor and water adsorption of polyimide films. *J. Mater. Chem. C* **11**, 10274–10281 (2023).
42. Hasegawa, M. & Hishiki, T. Poly(ester imide)s possessing low coefficients of thermal expansion and low water absorption (v). effects of ester-linked diamines with different lengths and substituents. *Polymers* **12**, 859 (2020).
43. Biswas, S. et al. Integrated multilayer stretchable printed circuit boards paving the way for deformable active matrix. *Nat. Commun.* **10**, 4909 (2019).
44. Zhong, A., Li, J., Zhang, G. & Sun, R. Adhesion and interface studies of the structure-controlled polyimide with smooth copper for high-frequency communication. *Adv. Mater. Interfaces* **9**, 2101745 (2022).
45. Li, H. et al. Fluorinated polyimide with triphenyl pyridine structure for 5G communications: Low dielectric, highly hydrophobic, and highly transparent. *Eur. Polym. J.* **197**, 112327 (2023).
46. Li, S. E. et al. Polyimide resins with superior thermal stability, dielectric properties, and solubility obtained by introducing trifluoromethyl and diphenylpyridine with different bulk pendant groups. *Polymer* **283**, 126245 (2023).
47. Yin, Q. et al. Reducing Intermolecular Friction Work: Preparation of Polyimide Films with Ultralow Dielectric Loss from MHz to THz Frequency. *Ind. Eng. Chem. Res.* **61**, 17894–17903 (2022).
48. Peng, W., Lei, H., Qiu, L., Bao, F. & Huang, M. Perfluorocyclobutyl-containing transparent polyimides with low dielectric constant and low dielectric loss. *Polym. Chem.* **13**, 3949–3955 (2022).
49. Zhong, M. et al. Organosoluble polyimides with low dielectric constant prepared from an asymmetric diamine containing bulky m-trifluoromethyl phenyl group. *React. Funct. Polym.* **169**, 105065 (2021).
50. Li, H. et al. Sustainable dielectric films with ultralow permittivity from soluble fluorinated polyimide. *Molecules* **28**, 3095 (2023).
51. Wang, Z.-h, Fang, G.-Q., He, J.-j, Yang, H.-x & Yang, S.-y Semi-aromatic thermosetting polyimide resins containing alicyclic units for achieving low melt viscosity and low dielectric constant. *React. Funct. Polym.* **146**, 104411 (2020).
52. Zhang, Y., He, J. & Yang, R. Ultra-low dielectric constant and high thermal stability of low-crosslinked polyimide with zinc tetraamino phthalocyanine. *J. Mater. Sci.* **57**, 16064–16079 (2022).

Acknowledgements

This work was supported financially by the National Natural Science Foundation of China (Key Program 52233016 and 51733007). The authors thank the hzwtech Co., Ltd for High-Performance Computing (CHPC) for providing computing software and the cluster facility for performing the computational work.

Author contributions

C.Z. and Q.L. conceived and designed the research. C.Z. performed the fabrication, characterization, and measurements. C.Z. and X.H. performed simulation calculations and the data analysis. C.Z. and Q.L. analyzed the mechanism. All authors contributed to manuscript preparation and wrote the manuscript. Q.L. supervised the project.

Competing interests

The authors declare that they have no known competing financial interests or personal relationships that could have appeared to influence the work reported in this paper.

Additional information

Supplementary information The online version contains supplementary material available at https://doi.org/10.1038/s43246-024-00502-7.

Correspondence and requests for materials should be addressed to Qinghua Lu.

Peer review information *Communications Materials* thanks Hai-Xia Yang, Feng Bao, Gaohui Sun and the other, anonymous, reviewer(s) for their contribution to the peer review of this work. Primary Handling Editors: Jet-Sing Lee. A peer review file is available.